

# 1 PEDIA: Prioritization of Exome Data by Image Analysis

2  
3 Hsieh, Tzung-Chien<sup>1,2,\*</sup>; Mensah, Martin Atta<sup>2,41\*</sup>; Pantel, Jean Tori<sup>1,2,41,\*</sup>; Krawitz, Peter<sup>1,+</sup>;  
4 and the PEDIA consortium  
5 PEDIA consortium: Aguilar, Dione<sup>3</sup>; Bar, Omri<sup>4</sup>; Bayat, Allan<sup>5</sup>; Becerra-Solano, Luis<sup>6</sup>; Bentzen,  
6 Heidi Beate<sup>7</sup>; Biskup, Saskia<sup>8</sup>; Borisov, Oleg<sup>1</sup>; Braaten, Oivind<sup>7</sup>; Ciaccio, Claudia<sup>9</sup>; Coutelier,  
7 Marie<sup>2</sup>; Cremer, Kirsten<sup>10</sup>; Danyel, Magdalena<sup>2</sup>; Daschkey, Svenja<sup>11</sup>; David-Eden, Hilda<sup>4</sup>;  
8 Devriendt, Koenraad<sup>12</sup>; Dölken, Sandra<sup>13</sup>; Douzgou, Sofia<sup>14</sup>; Đukić, Dejan<sup>1</sup>; Ehmke, Nadja<sup>2</sup>;  
9 Fauth, Christine<sup>15</sup>; Fischer-Zirnsak, Björn<sup>2</sup>; Fleischer, Nicole<sup>4</sup>; Gabriel, Heinz<sup>16</sup>; Graul-  
10 Neumann, Luitgard<sup>2</sup>; Gripp, Karen W.<sup>17</sup>; Gurovich, Yaron<sup>4</sup>; Gusina, Asya<sup>18</sup>; Haddad,  
11 Nechama<sup>2</sup>; Hajjir, Nurulhuda<sup>2</sup>; Hanani, Yair<sup>4</sup>; Hertzberg, Jakob<sup>2</sup>; Hoertnagel, Konstanze<sup>8</sup>;  
12 Howell, Janelle<sup>19</sup>; Ivanovski, Ivan<sup>20</sup>; Kaindl, Angela<sup>21</sup>; Kamphans, Tom<sup>22</sup>; Kamphausen,  
13 Susanne<sup>23</sup>; Karimov, Catherine<sup>24</sup>; Kathom, Hadil<sup>25</sup>; Keryan, Anna<sup>24</sup>; Khalil, Salma-Gamal<sup>2</sup>;  
14 Knaus, Alexej<sup>1</sup>; Köhler, Sebastian<sup>26</sup>; Kornak, Uwe<sup>2</sup>; Lavrov, Alexander<sup>27</sup>; Leitheiser,  
15 Maximilian<sup>2</sup>; Lyon, Gholson J.<sup>28</sup>; Mangold, Elisabeth<sup>29</sup>; Marín Reina, Purificación<sup>30</sup>; Martinez  
16 Carrascal, Antonio<sup>31</sup>; Mitter, Diana<sup>32</sup>; Morlan Herrador, Laura<sup>33</sup>; Nadav, Guy<sup>4</sup>; Nöthen,  
17 Markus<sup>10</sup>; Orrico, Alfredo<sup>34</sup>; Ott, Claus-Eric<sup>2</sup>; Park, Kristen<sup>35</sup>; Peterlin, Borut<sup>36</sup>; Pölsler,  
18 Laura<sup>15</sup>; Raas-Rothschild, Annick<sup>37</sup>; Revencu, Nicole<sup>38</sup>; Ringmann Fagerberg, Christina<sup>39</sup>;  
19 Robinson, Peter Nick<sup>40</sup>; Rosnev, Stanislav<sup>2</sup>; Rudnik, Sabine<sup>15</sup>; Rudolf, Gorazd<sup>36</sup>; Schatz,  
20 Ulrich<sup>15</sup>; Schossig, Anna<sup>15</sup>; Schubach, Max<sup>41</sup>; Shanoon, Or<sup>4</sup>; Sheridan, Eamonn<sup>42</sup>; Smirin-  
21 Yosef, Pola<sup>43</sup>; Spielmann, Malte<sup>44</sup>; Suk, Eun-Kyung<sup>45</sup>; Sznajer, Yves<sup>46</sup>; Thiel, Christian  
22 Thomas<sup>47</sup>; Thiel, Gundula<sup>45</sup>; Verloes, Alain<sup>48</sup>; Vrecar, Irena<sup>36</sup>; Wahl, Dagmar<sup>49</sup>; Weber,  
23 Ingrid<sup>15</sup>; Winter, Korina<sup>2</sup>; Wiśniewska, Marzena<sup>50</sup>; Wollnik, Bernd<sup>51</sup>; Yeung, Ming Wai<sup>1</sup>; Zhao,  
24 Max<sup>2</sup>; Zhu, Na<sup>2</sup>; Zschocke, Johannes<sup>15</sup>; Mundlos, Stefan<sup>2</sup>; Horn, Denise<sup>2</sup>

25 1 Institute of Genomic Statistics and Bioinformatics, University of Bonn, Bonn, Germany

26 2 Charité – Universitätsmedizin Berlin, corporate member of Freie Universität Berlin,  
27 Humboldt-Universität zu Berlin, and Berlin Institute of Health, Institute of Medical Genetics  
28 and Human Genetics, Berlin, Germany

29 3 Monterrey Institute of Technology and Higher Education, Mexico

30 4 FDNA Inc., Boston Massachusetts, United States

31 5 Rigshospitalet, Department of Neurology, Copenhagen, Denmark

32 6 Unidad de Investigación Médica en Medicina Reproductiva, Mexico

33 7 University of Oslo, Oslo, Norway

34 8 CeGaT GmbH, Tübingen, Germany

35 9 University of Milan, Milan, Italy

36 10 Department of Human Genetics, University Hospital of Bonn, Bonn, Germany

37 11 Heinrich Heine University Düsseldorf, Düsseldorf, Germany

38 12 Catholic University Leuven, Leuven, Belgium

39 13 University of Hamburg, Hamburg, Germany

40 14 University of Manchester, Manchester, United Kingdom

41 15 Division of Human Genetics, Medical University of Innsbruck, Innsbruck, Austria

42 16 University of Tübingen, Tübingen, Germany

43 17 A. I. duPont Hospital for Children, Wilmington, United States

44 18 National Research and Applied Medicine Centre “Mother and Child”, Belarus

45 19 Lineagen, United States

46 20 Santa Maria Nuova Hospital, Italy

47 21 Center for Chronically Sick Children (Sozialpädiatrisches Zentrum, SPZ), Charité -  
48 Universitätsmedizin Berlin, Berlin, Germany

49 22 GeneTalk, Bonn, Germany  
50 23 University Hospital Magdeburg, Magdeburg, Germany  
51 24 Children's Hospital of Los Angeles, Los Angeles, United States  
52 25 Medical University of Sofia, Sofia, Bulgaria  
53 26 Charité – Universitätsmedizin Berlin, corporate member of Freie Universität Berlin,  
54 Humboldt-Universität zu Berlin, and Berlin Institute of Health, NeuroCure Clinical Research  
55 Center, Berlin, Germany  
56 27 Research Institute of Medical Genetics of Russian Academy of Medical Sciences, Russian  
57 Federation  
58 28 Cold Spring Harbor Laboratory, Woodbury, United States  
59 29 University of Bonn, Bonn, Germany  
60 30 Hospital General Universitario De Valencia, Valencia, Spain  
61 31 Hospital General De Requena, Servicio Pediatría, Spain  
62 32 University Hospital Leipzig, Leipzig, Germany  
63 33 Hospital Universitario Miguel Servet, Spain  
64 34 Azienda Ospedaliera Universitaria Senese, Siena, Italy  
65 35 Children's Hospital Colorado, United States  
66 36 Clinical Institute of Medical Genetics, University Medical Centre Ljubljana, Ljubljana,  
67 Slovenia  
68 37 Sheba Medical Center, Israel  
69 38 Université Catholique de Louvain, Bruxelles, Belgium  
70 39 Odense University Hospital, Odense, Denmark  
71 40 The Jackson Laboratory for Genomic Medicine, Farmington, United States  
72 41 Berlin Institute of Health (BIH), Anna-Louisa-Karsch 2, 10178 Berlin, Germany  
73 42 School of Medicine, University of Leeds, Leeds, United Kingdom  
74 43 Ariel University, Ariel, Israel  
75 44 Department of Genome Sciences, University of Washington, Seattle, United States  
76 45 Center for Prenatal Diagnosis and Human Genetics, Berlin, Germany  
77 46 Cliniques universitaires Saint Luc UCL, Bruxelles, Belgium  
78 47 Institute of Human Genetics, Friedrich-Alexander-Universität Erlangen-Nürnberg FAU,  
79 Erlangen, Erlangen, Germany  
80 48 Hopital Robert Debré, Paris, France  
81 49 Center for Human Genetics and Laboratory Diagnostics, Germany  
82 50 Poznań University of Medical Sciences, Poznań, Poland  
83 51 University Medical Center Göttingen, Göttingen, Germany  
84 \* equally contributing first authors  
85 + corresponding author, [pkrawitz@uni-bonn.de](mailto:pkrawitz@uni-bonn.de)  
86

87 **Abstract**

88 **Phenotype information is crucial for the interpretation of genomic variants. So far it has only**  
89 **been accessible for bioinformatics workflows after encoding into clinical terms by expert**  
90 **dysmorphologists. Here, we introduce an approach, driven by artificial intelligence that uses**  
91 **portrait photographs for the interpretation of clinical exome data. We measured the value**  
92 **added by computer-assisted image analysis to the diagnostic yield on a cohort consisting of**  
93 **679 individuals with 105 different monogenic disorders. For each case in the cohort we**  
94 **compiled frontal photos, clinical features and the disease-causing mutations and simulated**  
95 **multiple exomes of different ethnic backgrounds. With the additional use of similarity**  
96 **scores from computer-assisted analysis of frontal photos, we were able to achieve a top-10-**  
97 **accuracy rate for the disease-causing gene of 99 %. As this performance is significantly**  
98 **higher than without the information from facial pattern recognition, we make gestalt scores**  
99 **available for prioritization via an API.**

100

101 Rare diseases affect approximately 6% of the population, with genetic syndromes accounting for about  
102 80 %.<sup>1,2</sup> The more than 5,000 entities represent a heterogeneous group of diseases, differing in cause,  
103 symptoms, and treatment, making diagnosis an important yet challenging healthcare issue. Due to  
104 extensive clinical variability this is true even for well characterized syndromes.<sup>1,3</sup>

105 Worldwide, more than half a million children born per year have a rare genetic disorder that is suitable  
106 for a diagnostic workup by exome sequencing, which has an unprecedented diagnostic yield for many  
107 indications such as developmental delay.<sup>4-9</sup> The main remaining concern for the integration of exome  
108 sequencing into clinical routine is to increase the efficiency of genetic variant interpretation. Making  
109 phenotypic information – the observable, clinical presentation – computer-readable is key in solving  
110 this problem, and in providing clinicians with a much-needed tool for diagnosing genetic syndromes.<sup>10</sup>

111 To date, the most advanced exome prioritization algorithms combine deleteriousness scores for  
112 mutations with semantic similarity searches of the clinical description of a patient.<sup>11-15</sup> The human  
113 phenotype ontology (HPO) with its extensive vocabulary has become the *lingua franca* for this  
114 purpose.<sup>16</sup> However, semantic similarity searches presuppose that facial features can be named. A  
115 facial gestalt that is simply described in the literature as *typical* or *characteristic* of a certain disease is  
116 of little help for these approaches.

117 Beyond language, capturing indicative patterns by deep-learning approaches has recently gained  
118 attention in assessing facial dysmorphism.<sup>17-21</sup> Artificial neural networks are now able to quantify the  
119 similarities of patient photos to hundreds of disease entities and achieve accuracies that match or even  
120 surpass the level of dysmorphologists in certain tasks.<sup>22-25</sup> For this reason tools such as Face2Gene are  
121 now used in addition to human expertise to guide the molecular testing and to interpret sequence  
122 variants. Here we investigate systematically whether facial image analysis can improve the evaluation  
123 of exome data and qualifies as a next-generation phenotyping technology for next-generation  
124 sequencing.<sup>26</sup>

125 **Results**

126 We first present an overview about the approach to prioritize exome data by image analysis (PEDIA);  
127 a detailed description is provided in the Methods.

128

129 **PEDIA classifier.** For the assessment of genetic variants, different sources of evidence have to be  
130 considered, from a populational, molecular, and phenotypic level. PEDIA is a Bayesian heuristic, that

131 can be used to update the probability that a mutation in a gene is disease-causing, given the  
132 phenotypic information contained in a frontal photograph.

133 To build this classifier, we first measured the similarities of the facial gestalt to 216 specific diseases in  
134 679 individuals with the convolutional neural network DeepGestalt.<sup>21</sup> By this means, we were able to  
135 acquire scores for disorders with a single genetic etiology that quantify the PP4 criteria of the ACMG  
136 guidelines which is used for variant interpretation.<sup>27,28</sup>

137 In addition to DeepGestalt, we computed further prediction scores that are widely used on clinical  
138 features (Phenomizer, Boqa, Feature) and genetic variants (CADD) for all individuals of the PEDIA  
139 cohort (Supplemental Table 1).<sup>29,30,31</sup> With this data set we trained and tested a support vector  
140 machine that can be used to prioritize the genetic variants in a VCF files from exome sequencing.

141 **Gene prioritization.**

142 The term next-generation sequencing (NGS) implies the interrogation of all genes in a single assay.  
143 Similarly, the term next-generation phenotyping (NGP) refers to technology enabling similarity  
144 searches on a large set of disorders based on clinical patient records and medical imaging data. In order  
145 to increase the efficiency in diagnostics, we combined both approaches and benchmarked gene  
146 prioritization.

147 Similar to the performance readout in Gurovich et al., the identification of the disease-gene in exome  
148 data also represents a multiclass classification problem and the number of sequence variants in the  
149 coding part of the genome illustrates the complexity of the diagnostic assessment. In reference guided-  
150 resequencing, about 20,000-30,000 single nucleotide variants and small indels have to be considered.  
151 Although the majority of these variants can be removed as benign polymorphisms, rare and potentially  
152 disease-causing mutations in more than 100 genes remain in a typical case with a suspected  
153 monogenic disorder. When only a deleteriousness score such as CADD is used to rank these mutations,  
154 the disease-causing gene is in the top 10 in less than 46 % of the cases of the PEDIA cohort. This  
155 performance increases to a top-10-accuracy rate of up to 88 %, when semantic similarity scores are  
156 included that are based on HPO feature annotations. These prioritization approaches also represent  
157 the current state of the art in diagnostic laboratories for single exomes.<sup>13,14</sup> The additional information  
158 contained in frontal photos of dysmorphic cases pushes the correct disease-gene to the top-10 in more  
159 than 99 % of the cases in the PEDIA cohort and in the DeepGestalt test set (Figure 1 B).

160 The value of a frontal photograph can exemplarily be demonstrated by a case with Coffin-Siris  
161 syndrome that is shown in Figure 2 A: The characteristic facial features are relatively mild, so the  
162 correct diagnosis is only listed as the third suggestion by DeepGestalt. Amongst all the variants  
163 encountered in an exome data set, the disease-causing gene *ARID1B* would only achieve rank 24, if  
164 scored by the molecular information alone. However, in synopsis with the phenotypic information, the  
165 PEDIA approach lists this gene as first candidate by far (Figure 2 C).

166 Although the syndrome of the case shown in Figure 2 might also be molecularly confirmed by a  
167 directed single gene test in other instances where the facial gestalt is more indicative, the high  
168 phenotypic variability associated with disease-causing mutations is well-known for genes of syndromic  
169 disorders. It has been exhibited in the deciphering developmental disorders (DDD) project, that many  
170 such diagnoses were made only after exome sequencing.<sup>6</sup> This finding is also reflected by frontal image  
171 analysis of the entire PEDIA cohort with DeepGestalt alone that achieves a top-10-accuracy rate for  
172 the disease-causing gene of around 58 %.

173 The efficiency of a prioritization algorithm can also be measured by the area under the curve (AUC) of  
174 the disease-causing mutation versus its ranked position. The higher the AUC, the higher the diagnostic  
175 yield in a fixed amount of time that is spent on the analysis of sequence variants (Figure 3). Combining  
176 similarity scores from image analysis, phenotypic features and molecular deleteriousness achieves the  
177 best AUC on the PEDIA cohort and is therefore suited to speed up diagnostics.

178 The contribution from the different sources of evidence to the PEDIA score is also reflected by the  
179 relative weight of the deleteriousness of the mutation (0.44), all feature-based scores combined (0.25)  
180 and the results from image analysis by DeepGestalt (0.31) that can be derived from a linear SVM model.  
181 We therefore also conclude that the information contained in a frontal photograph of patient goes  
182 beyond, what clinical terms can capture.

## 183 Discussion

184 According to the current version of the Online Mendelian Inheritance of Man Catalog, mutations in  
185 about 4000 genes are linked to phenotypes that are often difficult to distinguish and diagnose by  
186 clinical features alone, making next-generation sequencing a key technology for their molecular  
187 confirmation. However, the size and high variability of the genome as well as the low prevalence of  
188 disease-causing variants – many of them occur *de novo* – explain why sequence data analysis of a single  
189 individual is still challenging and time consuming.<sup>5,6</sup>

190 The guidelines for variant classification in the laboratory follow a qualitative heuristic that combines  
191 distinct types of evidence (functional, population, phenotype, etc.) and is compatible with Bayesian  
192 statistics.<sup>32</sup> The advantage of such a framework is that continuous evidence types can be integrated  
193 into the classification system. While *in silico* predictions about a variant's pathogenicity have a  
194 relatively long history in bioinformatics and machine learning, the quantification of phenotypic raw  
195 data with systems of artificial intelligence just began. Analogous to a score for the deleteriousness of  
196 a gene variant, one can include the phenotypic similarity to a distinct syndrome caused by mutations  
197 in the respective gene.

198 We analyzed this approach in the PEDIA cohort, consisting of 679 cases and covering 105 distinct  
199 disorders mapping to 181 disease-genes. Among these disorders were 73 phenotypes for which the  
200 performance of facial image analysis alone has recently been evaluated.<sup>21</sup> Although the top-10-  
201 accuracies for gestalt- and PEDIA-scoring cannot be compared directly, both approaches operate on a  
202 similar order of phenotypes and genes, respectively. Adding suitable molecular information to 260  
203 cases from the DeepGestalt publication test set increased the correct disease-gene in the top 10 to  
204 about 99%, from 90% with only the phenotypic information. Considering only molecular information  
205 and clinical features, but without the results from image analysis, the correct disease gene would have  
206 only been placed in the top 10 in 62%. The genetic background, which might correspond to a different  
207 number of variant calls or higher load of deleterious mutations, had negligible influence on the  
208 performance.

209 The performance for the entire PEDIA cohort is comparable to the DeepGestalt test set. However,  
210 there are three important lessons learned from specific subgroups or cases achieving lower PEDIA  
211 ranks: 1) Although the convolutional neural network used for image analysis has been pretrained on  
212 real-world uncontrolled 2D images, patient photographs that were true frontal, of high resolution,  
213 with good lightening and contrast, and few artifacts such as glasses performed better. 2) Particularly  
214 rare diseases, or recently described disorders, for which the classifier's representation is based on a  
215 smaller training set, show a lower performance, even if experienced dysmorphologists would consider  
216 them highly distinguishable.<sup>24,34</sup> 3) Molecular pathway diseases, modeled as a single class, can be  
217 biased towards the prevailing gene if there is substructure in the phenotypic series, meaning there  
218 actually are gene-specific differences in the gestalt and complete heterogeneity is simply an  
219 approximation.<sup>25</sup> This applies also to microdeletion syndromes that can be caused by single gene  
220 mutations, such as Smith-Magenis syndrome, or any clinical presentation of a phenotype that is  
221 considered atypical.

222 The only way to overcome the biases of semantic similarity metrics as well as AI-driven image analysis  
223 that are due to limited cohort sizes, is sharing of the phenotypic data sets.

224 In conclusion, the PEDIA study documents that exome variant interpretation benefits from computer-  
225 assisted image analysis of facial photographs, particularly if dysmorphism has been stated in the  
226 clinical notes. By including similarity scores from DeepGestalt, we improved the top-10-accuracy rate  
227 considerably. AI-driven pattern recognition of frontal facial patient photographs is an example of next-  
228 generation phenotyping technology with proven clinical value in the interpretation of next-generation  
229 sequencing data.

230 As deep-learning advances in the assessment of other medical imaging data, it will be interesting to  
231 study how these classifiers affect variant interpretation separately and in aggregate.<sup>35,36</sup>

232 **Data and Code Availability**

233 PEDIA is freely available for academic use at <https://pedia-study.org> and the source code is available  
234 at <https://github.com/PEDIA-Charite>.

235

236 **Acknowledgements**

237 This work was funded by the Deutsche Forschungsgemeinschaft (KR 3985/7-3, KR 3985/6-1)

238 **Author contributions**

239 Conceived and designed the study and drafted the manuscript: T.C.H., M.A.M., J.T.P., and P.M.K.

240 Project Coordination: M.A.M., J.T.P., N.F.,

241 Acquired, analyzed, and interpreted the clinical data: A.D., L.B.S., A.B., S.B., O.B., A.M.C., C.C., M.C.,  
242 K.C., S.D., M.D., K.D., S.D., S.D., D.D., N.E., C.R.F., B.F.Z., H.G., K.G., Y.G., N.H., N.H., L.M.H., K.H., I.I.,  
243 J.H., A.K., C.K., H.K., S.K., A.K., A.K., U.K., A.L., M.L., G.L., E.M., D.M., A.O., K.P., B.P., L.P., P.M.R., N.R.,  
244 S.R., A.R.R., S.R., G.R., U.S., A.S., P.S.Y., E.K.S., M.S., Y.S., C.T., G.T., A.V., I.V., D.W., I.W., K.W., M.W.,  
245 B.W., M.W.Y., L.G.N., C.E.O.

246 Chief clinical data review: D.H.

247 Performed the Bioinformatics and statistical analysis: M.S., J.H., M.A.M., T.C.H., T.K., S.K., M.Z., N.Z.,  
248 O.B., G.N., Y.G., Y.H., O.S., H.D.E., J.T.P., S.G.K.

249 Critically revised the manuscript for important intellectual content. H.B.B., P.N.R., S.M., J.Z.,

250 **Competing interests**

251 N.F., H.D.E., Y.G., G.N., O.B., Y.H., are employees of FDNA Inc, T.K. is employee of GeneTalk GmbH.

252

253    References

- 254    1. Institute of Medicine, Board on Health Sciences Policy, Committee on Accelerating Rare  
255    Diseases Research and Orphan Product Development. *Rare Diseases and Orphan*  
256    Products: Accelerating Research and Development. National Academies Press; 2011.
- 257    2. Evans WR, Rafi I. Rare diseases in general practice: recognising the zebras among the  
258    horses. *Br J Gen Pract* 2016;66(652):550–1.
- 259    3. Schieppati A, Henter J-I, Daina E, Aperia A. Why rare diseases are an important medical  
260    and social issue. *Lancet* 2008;371(9629):2039–41.
- 261    4. de Ligt J, Willemsen MH, van Bon BWM, et al. Diagnostic exome sequencing in persons  
262    with severe intellectual disability. *N Engl J Med* 2012;367(20):1921–9.
- 263    5. Vissers LELM, Gilissen C, Veltman JA. Genetic studies in intellectual disability and  
264    related disorders. *Nat Rev Genet* 2016;17(1):9–18.
- 265    6. Deciphering Developmental Disorders Study. Prevalence and architecture of de novo  
266    mutations in developmental disorders. *Nature* 2017;542(7642):433–8.
- 267    7. Hu H, Kahrizi K, Musante L, et al. Genetics of intellectual disability in consanguineous  
268    families. *Mol Psychiatry* [Internet] 2018; Available from: <http://dx.doi.org/10.1038/s41380-017-0012-2>
- 269    8. Online Mendelian Inheritance in Man, OMIM®. McKusick-Nathans Institute of Genetic  
270    Medicine, Johns Hopkins University (Baltimore, MD) [Internet]. OMIM. [cited  
271    2018]; Available from: <https://omim.org/>
- 272    9. Stark Z, Schofield D, Alam K, et al. Prospective comparison of the cost-effectiveness of  
273    clinical whole-exome sequencing with that of usual care overwhelmingly supports early  
274    use and reimbursement. *Genet Med* 2017;19(8):867–74.
- 275    10. Biesecker LG, Green RC. Diagnostic clinical genome and exome sequencing. *N Engl J  
276    Med* 2014;370(25):2418–25.
- 277    11. Stark Z, Dashnow H, Lunke S, et al. A clinically driven variant prioritization framework  
278    outperforms purely computational approaches for the diagnostic analysis of singleton  
279    WES data. *Eur J Hum Genet* 2017;25(11):1268–72.
- 280    12. Pengelly RJ, Alom T, Zhang Z, Hunt D, Ennis S, Collins A. Evaluating phenotype-driven  
281    approaches for genetic diagnoses from exomes in a clinical setting. *Sci Rep*  
282    2017;7(1):13509.
- 283    13. Zemojtel T, Köhler S, Mackenroth L, et al. Effective diagnosis of genetic disease by  
284    computational phenotype analysis of the disease-associated genome. *Sci Transl Med*  
285    2014;6(252):252ra123.
- 286    14. Smedley D, Jacobsen JOB, Jäger M, et al. Next-generation diagnostics and disease-  
287    gene discovery with the Exomiser. *Nat Protoc* 2015;10(12):2004–15.
- 288    15. Singleton MV, Guthery SL, Voelkerding KV, et al. Phevor combines multiple biomedical  
289    ontologies for accurate identification of disease-causing alleles in single individuals and  
290    small nuclear families. *Am J Hum Genet* 2014;94(4):599–610.
- 291    16. Robinson PN, Köhler S, Bauer S, Seelow D, Horn D, Mundlos S. The Human Phenotype  
292    Ontology: a tool for annotating and analyzing human hereditary disease. *Am J Hum  
293    Genet* 2008;83(5):610–5.
- 294    17. Loos HS, Wieczorek D, Würtz RP, von der Malsburg C, Horsthemke B. Computer-based  
295    recognition of dysmorphic faces. *Eur J Hum Genet* 2003;11(8):555–60.
- 296    18. Boehringer S, Vollmar T, Tasse C, et al. Syndrome identification based on 2D analysis  
297    software. *Eur J Hum Genet* 2006;14(10):1082–9.
- 298    19. Boehringer S, Guenther M, Sinigerova S, Wurtz RP, Horsthemke B, Wieczorek D.  
299    Automated syndrome detection in a set of clinical facial photographs. *Am J Med Genet A*  
300    2011;155(9):2161–9.
- 301    20. Ferry Q, Steinberg J, Webber C, et al. Diagnostically relevant facial gestalt information  
302    from ordinary photos. *Elife* 2014;3:e02020.
- 303    21. Gurovich Y, Hanani Y, Bar O, et al. DeepGestalt - Identifying Rare Genetic Syndromes  
304    Using Deep Learning [Internet]. arXiv [cs.CV]. 2018; Available from:  
305    <http://arxiv.org/abs/1801.07637>

307 22. Basel-Vanagaite L, Wolf L, Orin M, et al. Recognition of the Cornelia de Lange  
308 syndrome phenotype with facial dysmorphology novel analysis. *Clin Genet*  
309 2016;89(5):557–63.

310 23. Liehr T, Acquarola N, Pyle K, et al. Next generation phenotyping in Emanuel and  
311 Pallister-Killian syndrome using computer-aided facial dysmorphology analysis of 2D  
312 photos. *Clin Genet* 2018;93(2):378–81.

313 24. Pantel JT, Zhao M, Mensah MA, et al. Advances in computer-assisted syndrome  
314 recognition and differentiation in a set of metabolic disorders [Internet]. 2017;Available  
315 from: <http://dx.doi.org/10.1101/219394>

316 25. Knaus A, Pantel JT, Pendziwiat M, et al. Characterization of glycosylphosphatidylinositol  
317 biosynthesis defects by clinical features, flow cytometry, and automated image analysis.  
318 *Genome Med* 2018;10(1):3.

319 26. Hennekam RCM, Biesecker LG. Next-generation sequencing demands next-generation  
320 phenotyping. *Hum Mutat* 2012;33(5):884–6.

321 27. Richards, S. et al. Standards and guidelines for the interpretation of sequence variants:  
322 a joint consensus recommendation of the American College of Medical Genetics and  
323 Genomics and the Association for Molecular Pathology. *Genet. Med.* 17, 405–424  
324 (2015).

325 28. Tavtigian SV, Greenblatt MS, Harrison SM, et al. Modeling the ACMG/AMP variant  
326 classification guidelines as a Bayesian classification framework. *Genet Med* [Internet]  
327 2018;Available from: <http://dx.doi.org/10.1038/gim.2017.210>

328 29. Köhler S, Schulz MH, Krawitz P, et al. Clinical diagnostics in human genetics with  
329 semantic similarity searches in ontologies. *Am J Hum Genet* 2009;85(4):457–64.

330 30. Bauer S, Köhler S, Schulz MH, Robinson PN. Bayesian ontology querying for accurate  
331 and noise-tolerant semantic searches. *Bioinformatics* 2012;28(19):2502–8.

332 31. Kircher M, Witten DM, Jain P, O’Roak BJ, Cooper GM, Shendure J. A general  
333 framework for estimating the relative pathogenicity of human genetic variants. *Nat Genet*  
334 2014;46(3):310–5.

335 32. Wright CF, McRae JF, Clayton S, et al. Making new genetic diagnoses with old data:  
336 iterative reanalysis and reporting from genome-wide data in 1,133 families with  
337 developmental disorders. *Genet Med* [Internet] 2018;Available from:  
338 <http://dx.doi.org/10.1038/gim.2017.246>

339 33. The 1000 Genomes Project Consortium. A global reference for human genetic variation.  
340 *Nature* 2015;526:68.

341 34. Dudding-Byth T, Baxter A, Holliday EG, et al. Computer face-matching technology using  
342 two-dimensional photographs accurately matches the facial gestalt of unrelated  
343 individuals with the same syndromic form of intellectual disability. *BMC Biotechnol*  
344 2017;17:90.

345 35. Webb S. Deep learning for biology. *Nature* 2018;554(7693):555–7.

346 36. Shen D, Wu G, Suk H-I. Deep Learning in Medical Image Analysis. *Annu Rev Biomed  
347 Eng* 2017;19:221–48.

348

349

## 350 Materials and Methods

### 351 Patients

352 We compiled a cohort of 679 patients with a Mendelian disorder to evaluate Prioritization of Exome  
353 Data by Image Analysis (PEDIA). For all cases in this cohort frontal facial photographs were available  
354 for analysis and clinical features were documented in HPO terminology.<sup>16</sup> The diagnoses of all  
355 individuals have previously been confirmed molecularly and are suitable for analysis by exome  
356 sequencing. In total, the cohort covers 105 different monogenic syndromes that are linked to 181  
357 different genes. Of the individuals in this cohort, 375 were published and 309 have not been previously  
358 reported (see Supplementary Appendix).

359 The study was approved by the ethics committees of the Charité - Universitätsmedizin Berlin and of  
360 the University of Bonn Medical Center. Written informed consent was provided by the patients or their  
361 guardians.

362 In addition to PEDIA data set, we analyzed a subset of the DeepGestalt study comprising all 260 cases  
363 of the publication set with monogenic syndromes which diagnosable by exome sequencing.<sup>21</sup>

364

### 365 Data Preparation

366 The facial images were analyzed with DeepGestalt (FDNA), a deep convolutional neural network that  
367 was trained on more than 17,000 patient images.<sup>21</sup> The results of this analysis are gestalt scores  
368 quantifying the similarity to 216 different rare phenotypes per individual. Although DeepGestalt is built  
369 as a framework that aims to learn from every additional case, we excluded all data of the PEDIA cohort  
370 from the model for benchmarking purposes in a similar manner as described in the original publication.  
371 In addition to the image analysis, we performed semantic similarity searches with the annotated HPO  
372 terms by Feature Match (FDNA), Phenomizer and BOQA.<sup>29,30</sup>

373 We filtered all sequence variants as described by Wright et al. and scored the remaining mutations for  
374 deleteriousness with CADD.<sup>31,32</sup> If no exome data was available, we spiked the disease-causing  
375 mutation into the exome data of a healthy individual from the 1000 Genomes Project.<sup>33</sup> This exome  
376 simulation was applied to the entire PEDIA cohort to assess the influence of the genetic background  
377 on the performance of our scoring approach.

378 For the variants remaining after filtering, we derived the similarity scores from image analysis and  
379 semantic similarity searches that were based on HPO feature annotations for the syndromes  
380 associated with the respective genes. If there were several syndromes linked to a single gene, the  
381 highest gestalt and feature scores were selected. Case data is represented as table with a variable  
382 number of lines representing genes and five columns for the different scores (Figure 1 B). All five scores  
383 with per line as well as the Boolean label disease gene “true” or “false” were used to train a classifier  
384 that yields a single value per gene, the PEDIA score, that can be used for prioritization (Figure 1 C). A  
385 detailed description of preprocessing and filtering, as well as all the annotated data, can be found in  
386 our code repository.

### 387 Gene prioritization

388 We used a support vector machine (SVM) to prioritize the disease-causing gene in each patient. First,  
389 we split the PEDIA cohort into a training and a test set. We used a linear kernel on the five scores to  
390 train the SVM and selected the hyperparameter C in the range from  $2^{-6}$  to  $2^{12}$  by performing internal  
391 5-fold cross-validation on the training set. The C with highest top-1 accuracy was selected for training  
392 linear SVM. We further benchmarked the performance of each case in the test set with this model.  
393 The distance of each gene to the hyperplane - defined as the PEDIA score - was used to rank the genes  
394 for the case. If the disease-causing gene was at the first position, we called it a top 1 match, or if it was  
395 amongst the first ten genes, we called it a top 10 match.

396 To evaluate the accuracy, we conducted a 10-fold cross-validation, that is, we split 679 cases into 10  
397 groups to minimize overfitting. For the 260 cases from the DeepGestalt publication test set, where  
398 exome diagnostics would be applicable, we randomly selected a patient from the PEDIA cohort with

399 the same diagnosis and replaced the entire gestalt scores per case. Thus, we were also able to analyze  
400 the influence of another large collection of patient images in the exome prioritization. In total, all  
401 experiments were conducted ten times and the achieved top-1 and top-10-accuracies were averaged.  
402 All training data as well as the classifier are available at <https://github.com/PEDIA-Charite> and  
403 <https://pedia-study.org>

404

405 Performance evaluation in a classification task

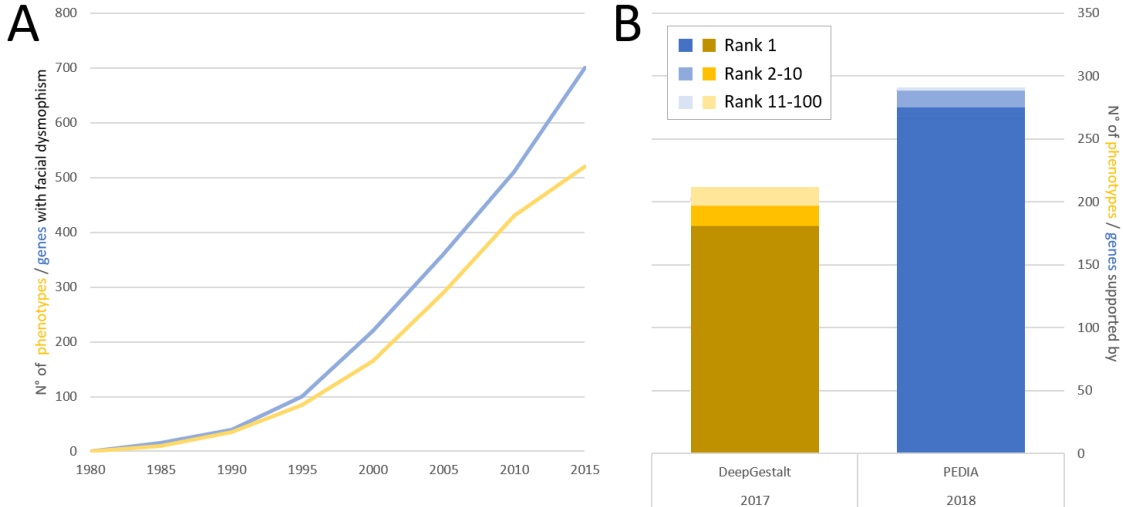
406 Both, DeepGestalt and PEDIA are approaches to solve multiclass classification problems (MCPs), the  
407 first tool operating on phenotypes and the second on genes. The difficulty of the task is characterized  
408 by the number of classes and the distinguishability of the different entities. For both MCPs the  
409 maximum number of classes can be estimated from Online Mendelian Inheritance in Man catalog, that  
410 is currently listing around 500 distinct disorders with facial abnormalities and 700 corresponding genes  
411 with disease-causing mutations (Figure 1 A).

412 Learning a phenotype in a neural network requires a certain number of unrelated cases. By the end of  
413 2017, DeepGestalt could distinguish between 216 different entities. Due to more training data, 60 new  
414 disorders were added in the last six months and the number is expected to increase further on.

415 The performance of a prioritization tool can be assessed by the proportion of cases in a test set for  
416 which the correct diagnosis or disease-gene is placed at the first position or amongst the first ten  
417 suggestions (top-1 and top-10-accuracy). The composition of the test set has an influence on the  
418 accuracy because some disease phenotypes are easier to recognize and some gene mutations are  
419 more readily identified as deleterious. The setup of the PEDIA cohort, which is comprehensively  
420 documented in the Supplementary Appendix, therefore aims at emulating the whole spectrum of cases  
421 that could currently be analyzed with DeepGestalt and diagnosed by exome sequencing.

422

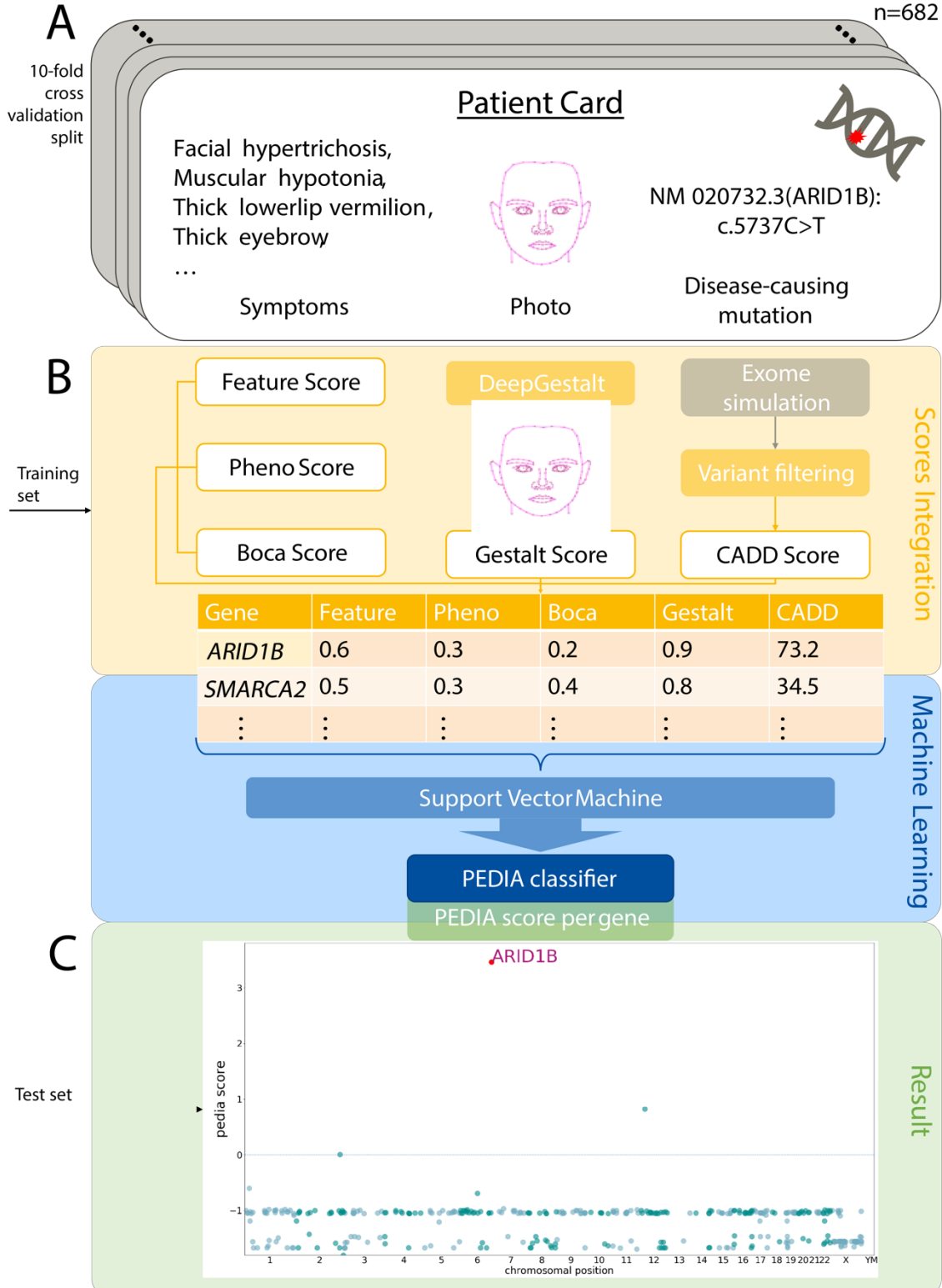
423



424

425 *Figure 1: A) Schematic Increase of Mendelian phenotypes with facial abnormalities and associated genes listed in the*  
426 *encyclopedia of Online Mendelian Inheritance in Man over time. B) The next-generation phenotyping tool DeepGestalt could*  
427 *be used to differentiate between 216 disorders in the end of 2017 and achieved a top-10-accuracy rate of 90 %. The subset*  
428 *of Mendelian phenotypes that are suitable for a diagnostic workup by exome sequencing corresponds to 290 genes and in*  
429 *the PEDIA cohort a top-1-accuracy of 98 % was achieved.*

430

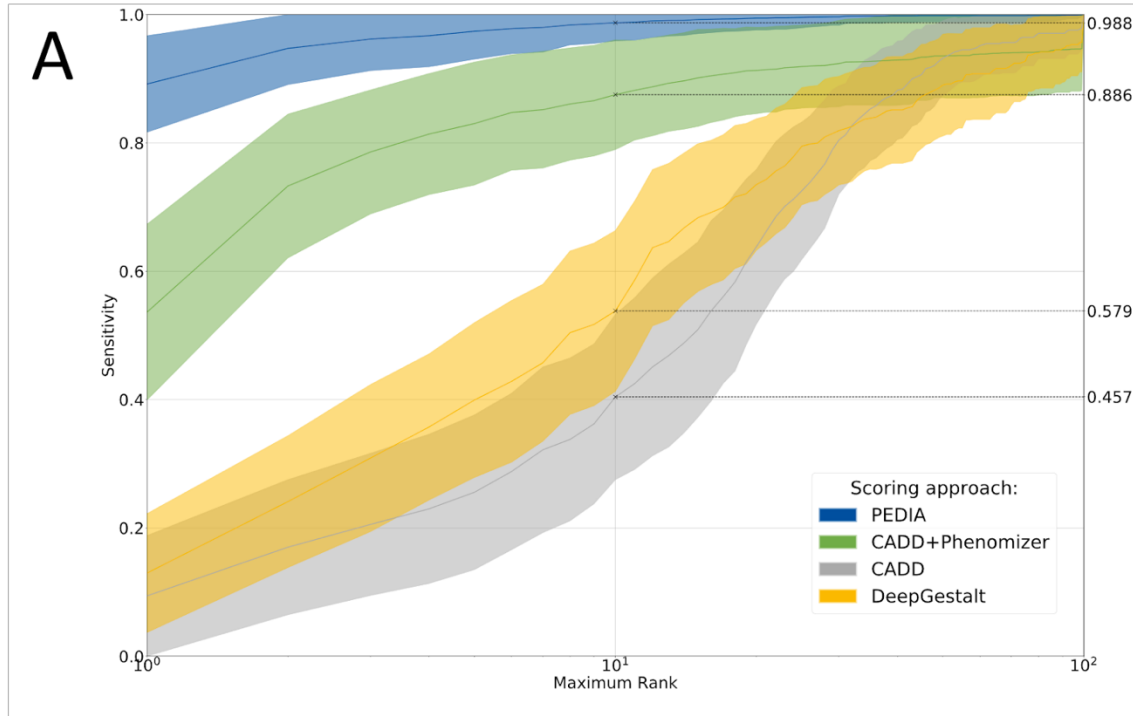


431

432

433 **Figure 2: Prioritization of Exome Data by Image Analysis.** A) Clinical features, facial photograph and disease-causing  
 434 mutation of one individual of the PEDIA cohort. In total the cohort consists of 679 cases with monogenic disorders that are  
 435 suitable for a diagnostic workup by exome sequencing. B) Clinical features, images and exome variants were evaluated  
 436 separately and integrated to a single score by a machine learning approach. C) The disease-causing gene of the case  
 437 depicted in A achieves the highest PEDIA score and molecularly confirms the diagnosis of Coffin-Siris syndrome. Other genes  
 438 associated with similar phenotypes such as Nicolaides-Baraitser syndrome, achieved also scores for gestalt but not for  
 439 variant deleteriousness. This figure has been adapted for bioRxiv by removing the patient photo. The original version with a  
 440 patient photo is available on request. Also see <https://pedia-study.org>

441



442

443 **Figure 3: Area under the curve for different disease-gene prioritization approaches.** For each case the exome variants are  
444 ordered according to four different scoring approaches, solely by a molecular deleteriousness score (C), by score from image  
445 analysis (DeepGestalt), by a combination of a molecular deleteriousness score and a clinical feature based semantic  
446 similarity score (P+C), or the PEDIA score that includes all three levels of evidence. The sensitivity of the prioritization  
447 approach depends on the number of genes that are considered in an ordered list. The top 10 accuracy rates of of Figure 1B  
448 correspond to the intersect of the curves for PEDIA and DeepGestalt at maximum rank  $10^1$ . Note that for benchmarking  
449 DeepGestalt on the gene level, syndrome similarity scores first have to be mapped to the gene level, resulting in a lower  
450 performance compared to the readout on a phenotype level, due to heterogeneity. The area under the curve is largest for  
451 PEDIA scoring. When e.g. the first ten candidate genes are considered, the syndromic similarity quantified by image analysis  
452 increases the sensitivity by about 20 % compared to P+C.